ACS Biomaterials SCIENCE & ENGINEERING

pubs.acs.org/journal/abseba

Letter

An Optogenetic Platform to Dynamically Control the Stiffness of Collagen Hydrogels

Erik Hopkins,[†] Eric Valois,[†] Alanna Stull, Kristy Le, Angela A. Pitenis, and Maxwell Z. Wilson*

Cite This: *ACS Biomater. Sci. Eng.* 2021, 7, 408−414

Read Online

ACCESS | Metrics & More | Article Recommendations | Supporting Information

ABSTRACT: The extracellular matrix (ECM) comprises a meshwork of biomacromolecules whose composition, architecture, and macroscopic properties, such as mechanics, instruct cell fate decisions during development and disease progression. Current methods implemented in mechanotransduction studies either fail to capture real-time mechanical dynamics or utilize synthetic polymers that lack the fibrillar nature of their natural counterparts. Here we present an optogenetic-inspired tool to construct light-responsive ECM mimetic hydrogels comprised exclusively of natural ECM proteins. Optogenetic tools offer seconds temporal resolution and submicron spatial resolution, permitting researchers to probe cell signaling dynamics with unprecedented precision. Here we demonstrated our approach of using SNAP-tag and its thiol-targeted substrate, benzylguanine-maleimide, to covalently attach blue-light-responsive proteins to collagen hydrogels. The resulting material (OptoGel), in addition to encompassing the native biological activity of collagen, stiffens upon exposure to blue light and softens in the dark. Optogels have immediate use in dissecting the cellular response to acute mechanical inputs and may also have applications in next-generation biointerfacing prosthetics.

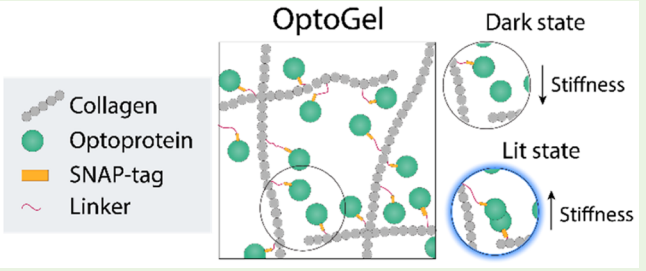

KEYWORDS: *optogenetics, dynamic ECM, collagen functionalization, "click" chemistry, ECM-mimetic substrate*

INTRODUCTION

Conventional hydrogels are passive scaffolds of synthetic or biological polymers largely utilized for their ability to interface with biological surfaces.[1] Their molecular architecture gives rise to macroscale properties, such as stiffness,[2] that determine their biological efficacy. Recently, there has been a growing appreciation for the importance of a surface's mechanical properties in steering the decision-making networks of an enormous range of cells and organisms.[3−6] Thus, the ability to tune the macroscale properties of hydrogels is crucial for their application in tissue engineering, cell culture, pharmaceuticals, diagnostics, implants, and, even contact lenses.[7]

The combined sensing of mechanical and chemical cues driving cell fate decisions during development and initiating cellular dysfunction in disease necessitates an extracellular environment that can precisely mimic the dynamic cellular boundary conditions that cells experience in vivo. Stimuli-responsive hydrogels made from naturally occurring ECM proteins, in which a user-defined input alters the chemical or mechanical functionality of the gel, can provide this ability in vitro. Previously, hydrogels have been engineered to stiffen, soften, or release embedded molecules as a result of chemically- or photo- induced restructuring of the polymer network.[8−10] Although such materials have unlocked the ability to acutely perturb the mechanical environment of cells, they either lack reversibility or are designed with synthetic polymers that form an amorphous, nonfibrillar, network. Thus, they fail to recapitulate the time-varying, chemically and structurally complex nature of the extracellular environment (ECM).[11−13]

The incorporation of photoswitchable proteins, whose binding state can be toggled with light, into synthetic hydrogel networks has resulted in bidirectionally dynamic materials.[14,15] Such hydrogels can cycle between material states in a light-dependent fashion, transmitting mechanical inputs to embedded cells. Recently, a synthetic polyethylene glycol (PEG) hydrogel functionalized with a red-light photoswitchable protein showed reversible mechanical activation.[14] Although such materials allow the study of dynamic mechanical inputs to cells, PEG is biologically inert and requires the addition of cell-recognition motifs to support cell growth.[16] Although the chemical nature of PEG (and other synthetic gel-forming polymers) facilitates such modifications, a widespread movement toward more physiologically relevant culture platforms highlights the need for an easily disseminatable method to control the mechanical properties of ECM mimetic substrates. Thus, to retain the biochemical and mechanical complexity of natural ECM, we sought to

Received: October 15, 2020
Accepted: December 29, 2020
Published: December 31, 2020

reversibly control the mechanical properties of a natural ECM-forming polymer.

Collagen type I is a ubiquitous hydrogel-forming protein that plays a key role in shaping ECM mechanics and signaling in vertebrates.[17] Post-translational modifications and a fibrillar structure give rise to intrinsic signaling capabilities essential for proper cell function.[6,18−20] Despite its relevance, collagen's utility is limited by its finite functionalization chemistries and low-yield recombinant purification.[21] Animal-extracted collagen is easily attainable and commonly modified with cross-linking or mineralization agents to achieve hydrogels of desired stiffnesses;[3,22] however these mechanisms are unidirectional and tend to occupy cell recognition sites that diminish collagen's intrinsic bioactivity.[23]

Here we report a promising platform technology for creating reversible, stimuli-responsive ECM for any thiol containing biopolymer. The modular design consists of three constituent components. (i) A translational fusion between a photoswitchable protein and SNAP-tag enzyme (Opto-SNAP),[24] (ii) a thiol-containing biopolymer (rat tail collagen, Corning), and (iii) a targeted heterofunctional SNAP-tag substrate (benzylguanine-maleimide) (Figure 1A). We show that benzylguanine-maleimide (BG-Mal) covalently links Opto-SNAP proteins to a collagen hydrogel (OptoGel), offering an alternative to recombinant ECM modification. OptoGels dynamically mimic biologically relevant tissue stiffness changes, that can influence cell fate decisions in development and disease,[14,25] through blue light stimulation. The ease with which OptoGels are assembled and their ability to precisely mimic natural ECM may greatly facilitate cellular mechanical studies.

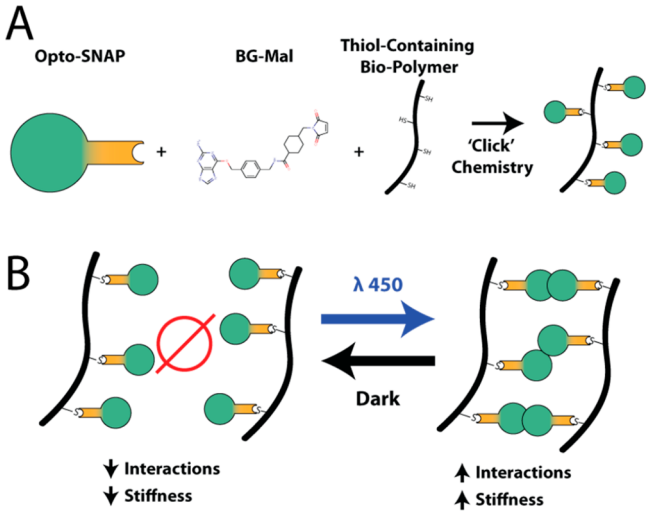

Figure 1. Polymer functionalization platform. (A) Three-piece functionalization platform consisting of a SNAP-tag fusion protein (Opto-SNAP), benzylguanine maleimide, and a cysteine-containing polymer. (B) Activation of Optoprotein-SNAP-tag fusion proteins, when attached to polymers through the aforementioned system, increases polymer−polymer interactions, thus stiffening the gel.

RESULTS

SNAP-tag Fusion Design. The core component of our OptoGels is a purified "optogenetic" protein that can occupy two self-association states, one with a substantially greater dissociation constant (K_d) than the other, depending on whether it has absorbed the energy from a photon of a particular wavelength of light.[26] To begin, we chose to work with the Lov-domain containing protein EL222, a blue-light-responsive protein from *Erythrobacter litoralis*.[27] EL222 undergoes a well-documented conformational rearrangement in the presence of blue light, whose switching efficiency peaks at 450 nm light, to expose a high-affinity homodimerization interface.[28] We hypothesized that covalently linking EL222 to gelled collagen by creating a SNAP-tag - EL222 fusion protein (EL222-SNAP) would permit light-programmable stiffening caused by the formation of nascent cross-links resulting from the light-induced decrease in EL222-EL222 K_d, as the EL222 homodimers would act analogously to cross-links (Figure 1B).

From the N- to C-terminus, EL222-SNAP consists of a 6× His tag to aid in purification, mCherry-FP to permit visualization of functionalized collagen hydrogels (OptoGel), a TEV cleavage site followed by EL222, a six-amino-acid GS linker, and the SNAP tag enzyme (Figure 2A, Table S1). The TEV cleavage site is intended to allow removal of the fluorescent reporter and aids in construct identification. This construct, EL222-SNAP, was expressed and purified through *E. coli* bacterial expression, metal affinity chromatography, and size exclusion chromatography. Correct expression was verified via Western blotting with anti-His and anti-SNAP-tag antibodies directed against the N- and C-termini, respectively. Colocalization of signal corresponding to anti-His and anti-

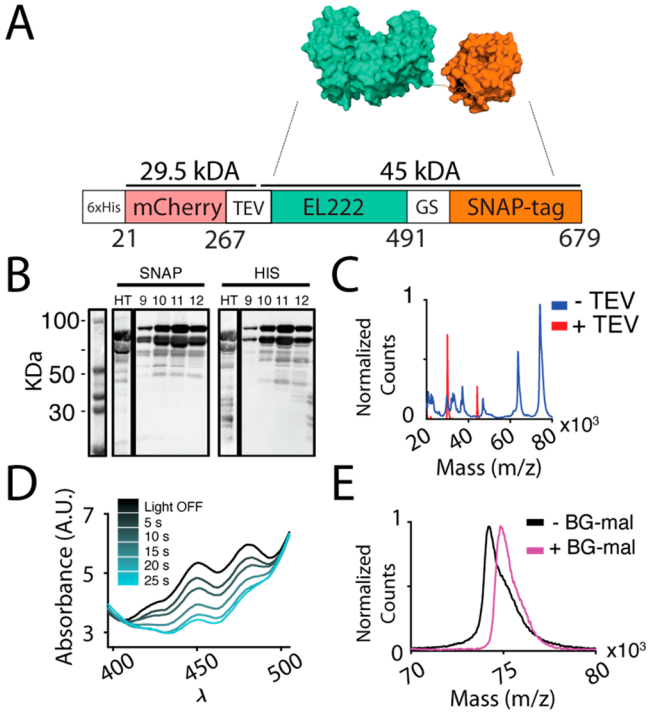

Figure 2. EL222-SNAP retains photoswitchability and BG-Mal reactivity. (A) EL222-SNAP fusion consisting of purification tag, mCherry, EL222, a GS linker, and SNAP-tag. (B) Western Blot analysis of purified EL222-SNAP (HT) and collected SEC fractions (9−12) with anti-SNAP (left) and anti-His (right) antibodies confirm the presence of a C-terminal SNAP-tag and N-terminal His-tag, respectively. (C) MALDI-TOF mass spectrometry of full-length EL222-SNAP (blue) and TEV-digested EL222-SNAP (red). ((D) Decrease in absorbance at 450 nm of EL222-SNAP during 25 s of blue light activation. (E) Mass increase of ∼650 Da of EL222-SNAP when incubated with BG-Mal.

https://dx.doi.org/10.1021/acsbiomaterials.0c01488
ACS Biomater. Sci. Eng. 2021, 7, 408−414

SNAP-tag at 75 kDa indicated the presence of a full-length construct (Figure 2B). Matrix-assisted laser desorption ionization time of flight mass spectrometry (MALDI-TOF MS) of purified EL222-SNAP produced a m/z peak at 74.4 (Figure 2C, red). An overnight TEV digestion of EL222-SNAP produced two distinct peaks at 30 and 44.2 (Figure 2C, blue), corresponding to the N- and C-terminal products of EL222-SNAP and confirming the successful purification of our synthetic product. We noted the presence of minor degradation products from the full-length product in both Western blots and MS (Figure 2B, C); however, these did not appear to influence EL222-SNAP function or subsequent experiments.

EL222-SNAP Functionality. Purified EL222-SNAP must both be light-responsive and efficiently conjugate BG-Mal in order to engineer reversible, light-tunable OptoGels. Thus, after purifying EL222-SNAP, we sought to verify that it was fully functional. In the absence of blue light, EL222-SNAP exhibits an absorbance peak at 450 nm, consistent with published reports of EL222.[28] Upon illumination, this peak decreased (Figure 2E), indicating that our recombinant EL222-SNAP could indeed photoactuate, consistent with Cys-FMN adduct formation and decreased K_d.[28] After removing blue light the 450 nm absorbance peak returned, indicating reversibility (Figure S1A). Additionally, we tested EL222-SNAP's capacity to be cyclically photo switched and found no fatigue after seven sequential activations (Figure S1B). Finally, measurements of photoswitchability of purified EL222-SNAP over 20 days revealed no degradation in its ability to respond to light activation (Figure S1E). Taken together, these results demonstrate that the light-responsive functionality of EL222 is retained in the SNAP-tag fusion.

In order for EL222-SNAP dimerization to alter the OptoGel's stiffness, it must be mechanically coupled through covalent attachment of the SNAP-tag domain to BG-Mal. To confirm this interaction, we compared MALDI-TOF mass spectrometry of EL222-SNAP with, and without, BG-Mal incubation. As expected, incubation with BG-Mal increased the mass of EL222-SNAP by 650 Da, consistent with the mass of BG-Mal (Figure 2D). TEV protease digestion of EL222-SNAP, which cleaves the His-mCherry from EL222-SNAP, confirmed BG-Mal binds at the C-terminal SNAP-tag (Figure S1C, D). Together, these results indicate that our purified EL222-SNAP has the functional characteristics required to engineer reversibly photoswitchable biopolymers.

Functionalization of Collagen Hydrogels with EL222-SNAP. After establishing the functionality of EL222-SNAP, we next sought to use this tool to functionalize off-the-shelf collagen hydrogels. Collagen is an ideal substrate to demonstrate this platform because of its ease of handling, ubiquitous use in cell culture and bioengineering,[11,29,30] and high mole ratio of cysteine residues (~17/molecule). This final attribute permits a high degree of functionalization via thiol-maleimide click chemistry between BG-Mal and collagen-residing cysteine residues.

The presence of solvent-accessible cysteine residues in collagen hydrogels was first assessed with Alexa555-maleimide. The strong fluorescent signal seen in Alexa555-modified hydrogels, even after multiple washes, indicated extensive availability of modification sites (Figure S2A). By utilizing BG-Mal as a directionally specific linker for SNAP-tag and thiols, a variety of Opto-SNAP fusion proteins can be tethered to the collagen network with equivalent maleimide−thiol click chemistry. We tested different BG-Mal concentrations to determine the most effective approach for attaching Opto-SNAPs. The 100 μM concentration was the only concentration resulting in a stiffness increase after completing functionalization and activation. Therefore, we used 100 μM BG-Mal for all subsequent experiments (Figure S2B). To avoid BG-Mal reacting with surface-exposed thiols on EL222, which could conjugate EL222-SNAP monomers and compromise their function, we incubated collagen hydrogels with BG-Mal prior to the addition of EL222-SNAP, resulting in specific, covalent coupling of EL222-SNAP to collagen (Figure S3). The resulting hydrogels showed mCherry fluorescence with clearly discernible collagen fibrils (Figure 3A, right). Hydrogels

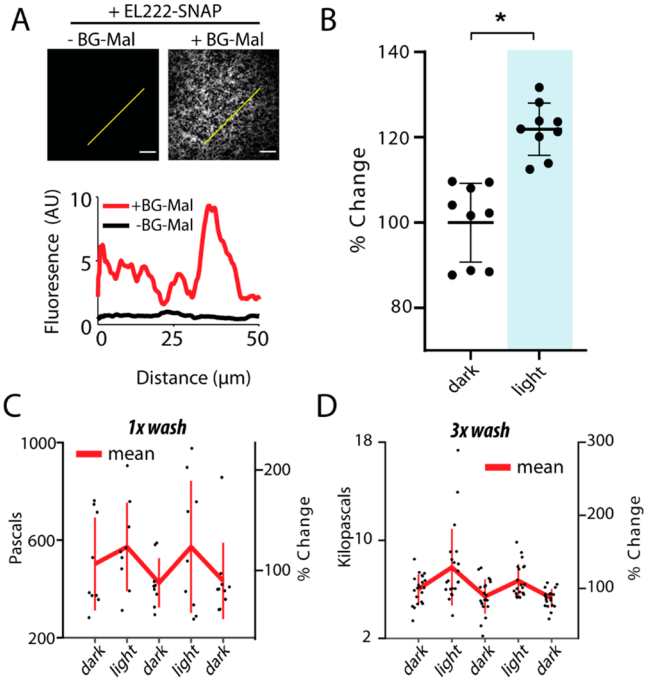

Figure 3. EL222-SNAP Binds and Alters Mechanical Properties of Collagen Hydrogel. (A) (Top) 1 mg/mL collagen hydrogel functionalized with EL222-SNAP with (right) and without (left) a prior BG-Mal incubation. mCherry signal, from EL222-SNAP, is shown. Scale bar = 10 μm. (Bottom) Fluorescence intensity across 50 μm trace (yellow line) of above images. (B) Percent change of elastic modulus, as determined by IT-AFM, of EL222 OptoGels during activation. * represents $p < 0.05$. (C) Elastic moduli of EL222 OptoGel during 2 sequential activations. (D) Elastic moduli of EL222 OptoGel made with 3 EL222-SNAP incubations (versus 1) during 2 sequential activations. Absolute averages for 3C and 3D reported in Table S2. Percent change is calculated from the mean.

incubated with EL222-SNAP but lacking BG-Mal, resulted in the absence of fluorescent fibrils (Figure 3A, left) demonstrating that EL222-SNAP coupling to collagen is BG-Mal dependent.

To establish OptoGels as a useful tool for cell mechanics studies, they must support cell growth in a similar manner to commonly used surfaces, such as collagen and glass. We confirmed that HeLa cells plated on EL222 OptoGels maintained a similar viability and metabolism to cells on collagen and glass substrates over a 7-day period, thus confirming that the EL222-SNAP functionalization is nontoxic (Figure S4).

https://dx.doi.org/10.1021/acsbiomaterials.0c01488
ACS Biomater. Sci. Eng. 2021, 7, 408−414

Light Dependent Mechanics of OptoGels. As discussed previously, EL222 undergoes a structural rearrangement when activated to expose a high-affinity dimerization site.[28] Notably, the relationship between cross-link density of collagen and resulting stiffness is well documented, and even exploited evolutionarily to yield tissues of varying mechanical properties.[2,31] Thus, we hypothesized that EL222-SNAP dimerization within OptoGels would act as reversible cross-links, therefore stiffening the OptoGel in the presence of light. To discern the stiffness dynamic range achievable with EL222 OptoGels, we subject them to blue light illumination while simultaneously measuring stiffness using IT-AFM. We found a statistically significant 22% increase in elastic modulus of EL222 OptoGels (196 to 239 Pa) (n = 9) (Figure 3B, Figure S5). To accurately mimic the mechanically dynamic environment experienced by cells in vivo, OptoGels must reversibly soften and stiffen in response to activating light. To test if OptoGels can be reversibly toggled, we subject them to two rounds of sequential activation (10 min OFF, 10 min ON). The elastic moduli of the OptoGel after illumination was roughly 20% higher than that of the preceding dark state, thus confirming that OptoGels can undergo dynamic stiffening (Figure 3C). To test if additional washes with purified EL222-SNAP increased the dynamic range, we tested the mechanical toggling in a gel that had been washed two additional times in EL222-SNAP for a total of 3 washes. While we found that these 3× OptoGels were an order of magnitude stiffer in their baseline dark state, upon activation they again stiffened to roughly 20% greater than their baseline (Figure 3D, Absolute values reported in Table S2). Interestingly, dark-state stiffnesses decreased with each successive activation in both OptoGels, most likely as a result of gel fatigue.

A well-established relationship between substrate stiffness and pore size has been gleaned from experiments conducted on static hydrogels. Typically, pore size can be tuned by altering polymer concentration or polymerization.[32,33] Therefore, to interrogate the mechanism of stiffening in activated EL222 OptoGels, we measured the pore size of an EL222 OptoGel with confocal microscopy pre- and post-activation. In the basal state (i.e., no illumination), the average pore area was measured to be 1.6 μm^2 (Figure S6). Despite blue-light activation, our visual quantification revealed no change in pore size; however, this method is limited to measuring changes greater than the resolution limit of our optical system.

DISCUSSION

The mechanical and biochemical importance of the ECM is well established and continues to be an area of intense research. Until recently, the inability to dynamically control the mechanical properties of protein-based hydrogels has forced these two parameters to be studied either independently or in a static fashion, thus inadequately recapitulating the dynamics of the extracellular environment.[34] As the most abundant protein in the ECM, collagen is an obvious choice for creating de novo ECM mimetic materials. Collagen's hierarchical structure provides many unique opportunities for tuning macroscopic mechanical properties.[11,29] Parameters such as fiber dimensions, polymerization condition, and fibrillar cross-link density can be manipulated prior to polymerization, yielding hydrogels with variable but static mechanical properties.[2,31,32] Considering these physical attributes are essential for many cell–scaffold interactions and mechanotransduction.[13,18−20] the field is limited to varying the properties of static gels and extrapolating between conditions to predict how cells would respond to in vivo. Although this approach has uncovered several relationships between substrate mechanics and cell fate decisions, it fails to capture real time changes that occur during development and disease.[3,4,6,35]

Our solution leverages the combined attributes from light-responsive proteins and the SNAP-tag enzyme. The resulting fusion protein has several key advantages for engineering ECM mimetic hydrogels. First, opto-proteins photoswitch within milliseconds of stimuli application,[36] allowing the ability to reversibly toggle material changes within physiologically relevant timeframes. Second, BG-Mal click chemistry makes for facile modification of most proteins via peptidyl thiols. Other commercially available benzylguanine derivates are designed to target carboxyl- or amine-functional groups, thus offering the possibility to engineer heterofunctionalized proteins and nonprotein-based ECM components, such as hyaluronic acid. In comparison to classical collagen cross-linking methods such as 1-ethyl-3-(3-dimthyllamino-propyl)-carbodiimide (EDC), thiol-maleimide click chemistry avoids compromising nucleophilic amines necessary for robust cell–substrate interactions.[37] Although the work presented here demonstrates the effects of homodimerization upon illumination, other classes of opto-proteins exist, including homo- and hetero-oligomerizers and dark-inducible protein complexes, offering a suite of options for engineering dynamic stimuli-responsive materials.[38−40]

By conjugating EL222 to collagen type 1, we were able to create a collagen hydrogel with programmable mechanical properties. While the first iteration of our OptoGels demonstrated a modest dynamic range (~22%) in comparison to other optoprotein-based dynamic substrates, who stiffen on the order of kilopascals,[14] such stiffness increases have been shown to increase integrin expression and drive invasion of mammary epithelial cells.[25] In future work we plan to increase the dynamic range of OptoGels by engineering Opto-SNAPs with increased oligomerization states (oligomeric vs dimeric); however, the aforementioned studies highlight potential immediate uses for OptoGels. Importantly, EL222 OptoGels underwent two rounds of reversible stiffening, highlighting their use in modeling complex mechanical dynamics. As previously mentioned, the relationship between mesh size and material stiffness has been well documented. Thus, we anticipated mesh network contraction during stimulation. Contrary to our prediction, increased stiffness appeared independent of mesh size. We interpreted this result to mean that EL222-SNAP was forming nascent cross-links between adjacent collagen fibrils, leading to increased cross-link density within the gel. Previous studies have shown such processes manifest increased stiffness independent of changes in pore size.[37,41,42] Future work may involve a combination of multiple cross-linking methods to first tune OptoGels to a desired baseline stiffness,[3,41] followed by functionalization to achieve dynamic control.

In summary, we describe an approach to create reversibly stiffening thiol-containing, biopolymer hydrogels using SNAP-tag coupling. As a proof of concept, we implemented this platform by coupling EL222-SNAP with type 1 collagen. We show that EL222-SNAP covalently binds collagen hydrogels in a BG-Mal dependent fashion and that the resulting hydrogel undergoes reversible increases in stiffness in a light-dependent fashion. Importantly, this technology combines collagen's intrinsic biological activity with the ability to tune mechanical

https://dx.doi.org/10.1021/acsbiomaterials.0c01488
ACS Biomater. Sci. Eng. 2021, 7, 408−414

properties, thus offering a user-regulated ECM-mimetic environment.

OptoGels provide an immediate opportunity to control acute mechanical cellular environments. Furthermore, by combining the existing OptoGel platform with advanced light delivery devices we hope to increase our control over the spatial and temporal dimensions. Additionally, by altering the "Opto" module of Opto-SNAP to include light inducible release of signaling proteins, we plan to expand the capabilities of OptoGels to include control of chemical cellular environments. Thus, OptoGels may serve as a singular material capable of recapitulating the mechanical and biochemical components of native ECM.

MATERIALS AND METHODS

Synthesis and Purification of EL222-SNAP Construct. The EL222-SNAP expression plasmid was synthesized from the pBAD expression vector (Invitrogen), mCherry, peblindv2 (encoding residues 1−225 of EL222), and pSNAP-tag(T7) (NEB) using Gibson Assembly. Plasmids were transformed into *E. coli* TOP10 (Thermo Fisher Scientific) and transformed clones were selected by 100 μg/mL ampicillin. To express EL222-SNAP, an overnight culture was used to inoculate 1 L of Terrific Broth (TB, IBI Scientific) supplemented with 100 μg/mL ampicillin such that the OD_{600} was 0.01. The culture was grown at 37 °C until the OD_{600} reached 0.4−0.6 at which point flasks were covered to keep the culture dark and 0.4% (w/v) arabinose was added to induce expression. *All steps after arabinose induction were carried out in the dark or under red light to prevent activation of EL222-SNAP.* After incubation at 25 °C for 14−16 h, bacteria were harvested by centrifugation, washed with 30 mL of PBS, and shock frozen in liquid nitrogen for future purification. To purify the EL222-SNAP, we put the frozen pellets through two freeze/thaw cycles and resuspended them in lysis buffer (20 mM imidazole, 20 mM Tris, 150 mM NaCl, pH 8.0) supplemented with 0.25 mg/mL lysozyme (Sigma, 6867−1G) and 1% (v/v) Protease Inhibitor Cocktail (Sigma, P8849−5 ML). After a 30 min incubation at room temperature with gentle shaking, the solution was sonicated at 30% power with an ON:OFF cycle of 15 s:45 s for a total time of 5 min. Cell lysates were clarified via centrifugation at 10 000g for 15 min. Clarified lysate was loaded onto a HiTrap high-performance Ni-NTA column (GE Healthcare) and separated using a BioRad NGC chromatography system (Bio-Rad Laboratories, Hercules CA). After sample loading, the column was washed with 5 column volumes of binding buffer (20 mM imidazole, 20 mM Tris and 150 mM NaCl pH 8.0) to remove unbound proteins. Proteins of interest were eluted from the column using binding buffer supplemented with imidazole (250 mM imidazole, 20 mM Tris and 150 mM NaCl pH 8) and quickly dialyzed to remove imidazole (20 mM Tris and 150 mM NaCl, pH 8.0). EL222-SNAP eluted from the His-Trap was further separated from unwanted proteins using a Superdex 75 10/300 GL size exclusion column. Five-hundred microliter of His-Trap elutant in dialysis buffer was loaded and separated using a flow rate of 400 μL/min while collecting 750 μL fractions. Protein concentration and purity were determined with ultraviolet absorption (λ = 280 nm, extinction coefficient 75 540 $M^{-1}cm^{-1}$ [Expasy protparam]) prior to aliquoting and freezing at −80 °C for future use.

Light Responsiveness of Purified EL222-SNAP. Purified EL222-SNAP was diluted to 0.5 mg/mL and subject to 1 min blue light OFF-ON cycles (7×). Absorbance spectra from 200 to 900 nm was measured at 5 s increments with an IMPLEN NP80 spectrophotometer. Blue light was delivered by a single 450 nm LED powered with a 9 V battery placed over the sample.

TEV Cleavage. Purified EL222-SNAP was diluted to 1 mg/mL and incubated with 1 μL TEV (2 mg/mL)(Sigma) in a 250 μL reaction. The sample was protected from light and digested overnight at room temperature. Cleaved samples were used for further characterization via mass spectrometry, incubation with BG-maleimide (NEB, S9153S), or loaded onto a HiTrap high-performance Ni-NTA column (GE Healthcare) for separation. For samples loaded into the affinity column, both the wash (Buffer A) and elutant (Buffer B) were saved, dialyzed into Buffer C, and examined with Western blot analysis using anti-His (SC Biotech, SC-53073) and anti-SNAP (NEB, P9310S) antibodies.

Additional samples, both TEV-treated and -untreated, were incubated with 100 μM BG-maleimide (NEB, S9153S) overnight at room temperature, and dialyzed into buffer C to remove excess BG-maleimide. Dialyzed samples were used for characterization with MALDI-TOF mass spectrometry.

OptoGel Handling and Preparation. To promote adhesion of collagen to glass surfaces for subsequent mechanical and cellular tests, surfaces were treated with silanol followed by glutaraldehyde. Briefly, 15 mm glass coverslips (#1.5) were cleaned in a bath of ethanol for 24 h and then dried in the oven at 155 °C for 1 h. Clean surfaces were in incubated in excess 2% 3-aminopropyl)triethoxysilane (Sigma-Aldrich) in ethanol for 1 h at room temperature will orbital shaking at 30 rpm. Surfaces were then rinsed with excess ethanol and heated at 37 °C overnight. Silanated surfaces were subsequently treated with 2% glutaraldehyde (Electron Microscopy Sciences, # 16216−10) in PBS for 2 h at room temp. Surfaces were then rinsed with excess PBS (2×) and deionized water (2×) to remove excess glutaraldehyde and salt and dried using a sterile air stream before being used to support hydrogels.

Collagen hydrogels were synthesized from rat-tail collagen (Corning, 354249) per the manufacturer's suggestion. Briefly, 1 mg/mL hydrogels (70 μL) were prepped from a high-concentration collagen stock (9.4 mg/mL), 1 M NaOH, 10× PBS and water. Hydrogel solution was incubated at 37 °C for 45 min to induce gelation. After gelation, hydrogels to be imaged with Alexa555-maleimide (Thermo) were incubated in 100 nM dye solution for 2 h at room temperature. Hydrogels were washed 3 times with PBS to remove unbound dye and stored at 4 °C until imaging.

Hydrogels to be functionalized to OptoGels were incubated in 100 μM BG-maleimide for 1 h at room temperature. Unbound BG-Mal was removed with 3× PBS washes. Hydrogels were further incubated in 4.5 mg/mL EL222-SNAP overnight at room temperature and washed the following day. *All opto protein incubations and proceeding steps were done in the dark to prevent aberrant opto-protein activation.* Hydrogels were stored submerged in the dark in PBS at 4 °C until experiments.

HeLa Cell Culture and Viability Assays. HeLa cells were stored at 37 °C and 5% CO in T25 flasks in Dulbecco's modified Eagle medium (DMEM) containing 10% fetal bovine serum and 1% antibiotic (25 units/mL penicillin, 25 μg/mL streptomycin)-(Invitrogen). For alamarBlue and Live/Dead assays, 96-well glass bottom dishes (Cellvis, Mountain View, CA) were salinated as previously described and 50 μL collagen hydrogels were cast in the bottom of the wells and functionalized with EL222-SNAP. Cells were plated at a density of 10 000 cells/well in and monitored over 7 days. Metabolic activity was visualized using media supplemented with 10% alamarBlue solution following manufacturers protocol. One-hundred microliter samples of media were taken after a 1 h incubation at 37 °C and fluorescence signal (Ex/Em 560 nm/590 nm) was read with a plate reader (Biotek). After incubation in alamarBlue-supplemented media, cells were washed with PBS, DMEM, and replenished with fresh media.

Live versus dead cells were quantified using a LIVE/DEAD viability/cytotoxicity kit (Thermo). Cells were washed once with PBS and incubated in 2 μM calcein-AM and 4 μM ethidium homodimer-1 for 45 min at 37 °C prior to imaging. Images were captured on a Nikon Super Resolution Spinning Disk Confocal microscope and live/dead cells were identified by custom FIJI macros or by hand, depending on cell density.

Pore Size Determination. EL222 OptoGels were visualized with a spinning disk super resolution confocal microscope (Nikon) with a 60× water-immersion lens and 1.5× multiplier. Gels were activated with 1 s pulses of 100% 447 nm laser every 5 s for 10 min mCherry on EL222-SNAP was utilized to visualize the microarchitecture of OptoGels. The hydrogel was visualized as 5 μM Z-stacks with slices

https://dx.doi.org/10.1021/acsbiomaterials.0c01488
ACS Biomater. Sci. Eng. 2021, 7, 408−414

every 0.3 μM (18 slices in total). Slices were taken with the following settings: 100% 561 nm laser, 100 ms exposure, sum of eight images. Images used for pore size determination were constructed from three adjacent slices combined as average intensity projections. Four different 40 μM × 40 μM areas, before and after activation, were analyzed in FIJI using elliptical ROIs to identify pores. Images were randomized to prevent biased between pre- and post-activation and subject to analysis by three individuals.

IT-AFM. Images and force measurements were conducted on a MFP-3D Bio (Asylum Research, Santa Barbara, CA). SICON-TL-SiO_2-A silicon tips with a 5 μm radius probe (APPNano, Mountain View, CA) were used in all experiments. Gels were cast onto 10 mm mica discs (TedPella, Inc.) glued to standard microscope slides. All experiments were conducted within 24 h of casting. Samples are loaded into the AFM scanning stage and subsequently submerged in PBS. Submerged samples were allowed to equilibrate in the instrument for 30 min. Prior to force measurements, the cantilever spring constant was experimentally determined by the thermal tune method usually ranging between 0.5 to 1 N/m. Deflection sensitivity was calculated using a glass slide as an indefinitely stiff calibrant material. Force spectroscopy measurements were conducted over the maximum piezo travel length at a 2 μm/s load/unload rate with a maximal loading force of 20 nN. Stiffness and values were calculated by Asylum Research's Elastic Analysis Tool by fitting the lower 10% of the loading curve, a probe radius of 5000 nm, and a Poisson ratio of 0.5 to the Hertz model.

MALDI-TOF Mass Spectrometry. EL222-SNAP identity was assessed using MALDI-TOF MS. Purified protein diluted to 1 mg/mL was mixed 1:10 with MALDI-matrix, a saturated solution of Sinapinic acid in 50% acetonitrile 1% trifluoroacetic acid. The protein solution was then applied to a 96 spot MALDI target plate (Bruker) and air-dried for 30 min. Mass spec analysis was conducted using a Microflex LRF MALDI-TOF (Bruker). Sample targets were irradiated using a nitrogen laser at 337 nm and a pulse length of 3 ns with a repetition rate of 20 Hz. Detection occurred in linear mode between 20 and 80 kDa at sampling rate of 1 Gs/s. Protein calibration standard 1 (Bruker #206355) was used as an internal calibration.

Sample Illumination. Photoswitching and AFM samples from experiments detailed in main text Figures 2 and 3 and Figures S1, S2, S5, and S6 were illuminated at a distance of 4 cm from the sample using a home-built blue LED resulting in a surface power density of approximately 10 mW/cm^2 at 450 nm. Light power was measured using a ThorLabs S121C photodiode power sensor with a 500 mW max rating.

Statistical Analysis. All scatter plots are presented as mean + standard deviation. Student *t* tests were performed on all data sets using the MatLab function *ttest2* with significance of $P < 0.05$ denoted by *.

■ ASSOCIATED CONTENT

Supporting Information

The Supporting Information is available free of charge at https://pubs.acs.org/doi/10.1021/acsbiomaterials.0c01488.

Photoswitchability and BG-Mal binding of EL222-SNAP; collagen Alexa555-maleimide staining; OptoGel production schematic; HeLa cell viability data; representative force−indentation curve; pore size data; EL222-SNAP amino acid sequence; sequential activation elastic moduli (PDF)

■ AUTHOR INFORMATION

Corresponding Author

Maxwell Z. Wilson − *Department of Molecular, Cellular, and Developmental Biology, Neuroscience Research Institute, and Center for BioEngineering, University of California, Santa Barbara, Santa Barbara, California 93106, United States;* orcid.org/0000-0002-2806-1919; Email: mzw@ucsb.edu

Authors

Erik Hopkins − *Department of Molecular, Cellular, and Developmental Biology, University of California, Santa Barbara, Santa Barbara, California 93106, United States*

Eric Valois − *Department of Molecular, Cellular, and Developmental Biology, Center for BioEngineering, and Materials Department, University of California, Santa Barbara, Santa Barbara, California 93106, United States;* orcid.org/0000-0002-6824-2933

Alanna Stull − *Department of Molecular, Cellular, and Developmental Biology, University of California, Santa Barbara, Santa Barbara, California 93106, United States*

Kristy Le − *Department of Molecular, Cellular, and Developmental Biology, University of California, Santa Barbara, Santa Barbara, California 93106, United States*

Angela A. Pitenis − *Materials Department, University of California, Santa Barbara, Santa Barbara, California 93106, United States*

Complete contact information is available at: https://pubs.acs.org/10.1021/acsbiomaterials.0c01488

Author Contributions

†E.H.and E.V. contributed equally to this work.

Notes

The authors declare no competing financial interest.

■ ACKNOWLEDGMENTS

The authors acknowledge support from the California Nanosystems Institute (CNSI), supported by the University of California, Santa Barbara, and the University of California, Office of the President. E.V. and A.A.P. were supported by the MRSEC Program of the National Science Foundation under Award DMR 1720256.

■ REFERENCES

(1) Peppas, N. A.; Hilt, J. Z.; Khademhosseini, A.; Langer, R. Hydrogels in Biology and Medicine: From Molecular Principles to Bionanotechnology. *Adv. Mater.* **2006**, *18*, 1345−1360.

(2) Lin, S.; Gu, L. Influence of Crosslink Density and Stiffness on Mechanical Properties of Type I Collagen Gel. *Materials* **2015**, *8*, 551−560.

(3) Di Caprio, N.; Bellas, E. Adipose Tissue Pathology: Collagen Stiffness and Architecture Regulate Fibrotic Gene Expression in Engineered Adipose Tissue. *Adv. Biosyst.* **2020**, *4*, 2070061.

(4) Seo, B. R.; Chen, X.; Ling, L.; Song, Y. H.; Shimpi, A. A.; Choi, S.; Gonzalez, J.; Sapudom, J.; Wang, K.; Andresen Eguiluz, R. C.; et al. Collagen microarchitecture mechanically controls myofibroblast differentiation. *Proc. Natl. Acad. Sci. U. S. A.* **2020**, *117*, 11387.

(5) Siryaporn, A.; Kuchma, S. L.; O'toole, G. A.; Gitai, Z. Surface attachment induces Pseudomonas aeruginosa virulence. *Proc. Natl. Acad. Sci. U. S. A.* **2014**, *111*, 16860−16865.

(6) Kawahara, K.; Yoshida, T.; Maruno, T.; Oki, H.; Ohkubo, T.; Koide, T.; Kobayashi, Y. Spatiotemporal regulation of PEDF signaling by type I collagen remodeling. *Proc. Natl. Acad. Sci. U. S. A.* **2020**, *117*, 11450.

(7) Laftah, W. A.; Hashim, S.; Ibrahim, A. N. Polymer Hydrogels: A Review. *Polym.-Plast. Technol. Eng.* **2011**, *50*, 1475−1486.

(8) Stowers, R. S.; Allen, S. C.; Suggs, L. J. Dynamic phototuning of 3D hydrogel stiffness. *Proc. Natl. Acad. Sci. U. S. A.* **2015**, *112*, 1953−1958.

(9) Wang, R.; Yang, Z.; Luo, J.; Hsing, I.-M.; Sun, F. B 12-dependent photoresponsive protein hydrogels for controlled stem cell/protein release. *Proc. Natl. Acad. Sci. U. S. A.* **2017**, *114*, 5912−5917.
(10) Yang, Z.; Yang, Y.; Wang, M.; Wang, T.; Fok, H. K. F.; Jiang, B.; Xiao, W.; Kou, S.; Guo, Y.; Yan, Y.; et al. Dynamically Tunable, Macroscopic Molecular Networks Enabled by Cellular Synthesis of 4-Arm Star-like Proteins. *Matter* **2020**, *2*, 233−249.
(11) Caliari, S. R.; Burdick, J. A. A practical guide to hydrogels for cell culture. *Nat. Methods* **2016**, *13*, 405−414.
(12) Hu, W.; Li, Q.; Li, B.; Ma, K.; Zhang, C.; Fu, X. Optogenetics sheds new light on tissue engineering and regenerative medicine. *Biomaterials* **2020**, *227*, 119546.
(13) Prince, E.; Kumacheva, E. Design and applications of man-made biomimetic fibrillar hydrogels. *Nat. Rev. Mater.* **2019**, *4*, 99−115.
(14) Horner, M.; Raute, K.; Hummel, B.; Madl, J.; Creusen, G.; Thomas, O. S.; Christen, E. H.; Hotz, N.; Gubeli, R. J.; Engesser, R.; et al. Phytochrome-Based Extracellular Matrix with Reversibly Tunable Mechanical Properties. *Adv. Mater.* **2019**, *31*, 1806727.
(15) Liu, L.; Shadish, J. A.; Arakawa, C. K.; Shi, K.; Davis, J.; DeForest, C. A. Cyclic Stiffness Modulation of Cell-Laden Protein-Polymer Hydrogels in Response to User-Specified Stimuli Including Light Dynamic Biomaterials. *Dyn. Biomater.* **2018**, *2*, 1800240.
(16) Kyburz, K. A.; Anseth, K. S. Synthetic Mimics of the Extracellular Matrix: How Simple is Complex Enough? HHS Public Access Author manuscript. *Ann. Biomed. Eng.* **2015**, *43*, 489−500.
(17) Yamauchi, M.; Sricholpech, M. Lysine post-translational modifications of collagen. *Essays Biochem.* **2012**, *52*, 113−133.
(18) Baker, B. M.; Trappmann, B.; Wang, W. Y.; Sakar, M. S.; Kim, I. L.; Shenoy, V. B.; Burdick, J. A.; Chen, C. S. Cell-mediated fibre recruitment drives extracellular matrix mechanosensing in engineered fibrillar microenvironments. *Nat. Mater.* **2015**, *14*, 1262−1270.
(19) Hynes, R. O. The extracellular matrix: Not just pretty fibrils. *Science* **2009**, *326*, 1216−1219.
(20) Lou, J.; Stowers, R.; Nam, S.; Xia, Y.; Chaudhuri, O. Stress relaxing hyaluronic acid-collagen hydrogels promote cell spreading, fiber remodeling, and focal adhesion formation in 3D cell culture. *Biomaterials* **2018**, *154*, 213−222.
(21) Ruggiero, F.; Koch, M. Making recombinant extracellular matrix proteins. *Methods* **2008**, *45*, 75−85.
(22) Roether, J.; Bertels, S.; Oelschlaeger, C.; Bastmeyer, M.; Willenbacher, N. Microstructure, local viscoelasticity and cell culture suitability of 3D hybrid HA/collagen scaffolds. *PLoS One* **2018**, *13*, e0207397.
(23) Grover, C. N.; Farndale, R. W.; Best, S. M.; Cameron, R. E. The interplay between physical and chemical properties of protein films affects their bioactivity. *J. Biomed. Mater. Res., Part A* **2012**, *100*, 2401−2411.
(24) Juillerat, A.; Gronemeyer, T.; Keppler, A.; Gendreizig, S.; Pick, H.; Vogel, H.; Johnsson, K. Directed Evolution of O 6-Alkylguanine-DNA Alkyltransferase for Efficient Labeling of Fusion Proteins with Small Molecules In Vivo. *Chem. Biol.* **2003**, *10*, 313−317.
(25) Levental, K. R.; Yu, H.; Kass, L.; Lakins, J. N.; Egeblad, M.; Erler, J. T.; Fong, S. F. T.; Csiszar, K.; Giaccia, A.; Weninger, W.; Yamauchi, M.; Gasser, D. L.; Weaver, V. M. Matrix Crosslinking Forces Tumor Progression by Enhancing Integrin Signaling. *Cell* **2009**, *139*, 891−906.
(26) Takakado, A.; Nakasone, Y.; Terazima, M. Photoinduced dimerization of a photosensory DNA-binding protein EL222 and its LOV domain †. *Phys. Chem. Chem. Phys.* **2017**, *19*, 24855.
(27) Zoltowski, B. D.; Motta-Mena, L. B.; Gardner, K. H. Blue Light-Induced Dimerization of a Bacterial LOV−HTH DNA-Binding Protein. *Biochemistry* **2013**, *52*, 6653−6661.
(28) Nash, A. I.; McNulty, R.; Shillito, M. E.; Swartz, T. E.; Bogomolni, R. A.; Luecke, H.; Gardner, K. H. Structural basis of photosensitivity in a bacterial light-oxygen-voltage/helix-turn-helix (LOV-HTH) DNA-binding protein. *Proc. Natl. Acad. Sci. U. S. A.* **2011**, *108*, 9499−9454.
(29) Meyer, M. Processing of collagen based biomaterials and the resulting materials properties. *Biomed. Eng. Online* **2019**, *18*, 24.
(30) Marques, C. F.; Diogo, G. S.; Pina, S.; Oliveira, J. M.; Silva, T. H.; Reis, R. L. Collagen-based bioinks for hard tissue engineering applications: a comprehensive review. *J. Mater. Sci.: Mater. Med.* **2019**, *30*, 1−12.
(31) Depalle, B.; Qin, Z.; Shefelbine, S. J.; Buehler, M. J. Influence of cross-link structure, density and mechanical properties in the mesoscale deformation mechanisms of collagen fibrils. *J. Mech. Behav. Biomed. Mater.* **2015**, *52*, 1−13.
(32) Yang, Y.-L.; Leone, L. M.; Kaufman, L. J. Elastic Moduli of Collagen Gels Can Be Predicted from Two-Dimensional Confocal Microscopy. *Biophys. J.* **2009**, *97*, 2051−2060.
(33) Taufalele, P. V.; VanderBurgh, J. A.; Munoz, A.; Zanotelli, M. R.; Reinhart-King, C. A. Fiber alignment drives changes in architectural and mechanical features in collagen matrices. *PLoS One* **2019**, *14*, e0216537.
(34) Geckil, H.; Xu, F.; Zhang, X.; Moon, S.; Demirci, U. Engineering hydrogels as extracellular matrix mimics. *Nanomedicine* **2010**, *5*, 469−484.
(35) Zhou, Q.; Lyu, S.; Bertrand, A. A.; Hu, A. C.; Chan, C. H.; Ren, X.; Dewey, M. J.; Tiffany, A. S.; Harley, B. A. C.; Lee, J. C. Stiffness of Nanoparticulate Mineralized Collagen Scaffolds Triggers Osteogenesis via Mechanotransduction and Canonical Wnt Signaling. *bioRxiv* **2020**, DOI: 10.1101/2020.03.09.982231.
(36) Iuliano, J. N.; Gil, A. A.; Laptenok, S. P.; Hall, C. R.; Tolentino Collado, J.; Lukacs, A.; Hag Ahmed, S. A.; Abyad, J.; Daryaee, T.; Greetham, G. M.; et al. Variation in LOV Photoreceptor Activation Dynamics Probed by Time-Resolved Infrared Spectroscopy. *Biochemistry* **2018**, *57*, 620−630.
(37) Roeder, B. A.; Kokini, K.; Sturgis, J. E.; Robinson, J. P.; Voytik-Harbin, S. L. Tensile Mechanical Properties of Three-Dimensional Type I Collagen Extracellular Matrices With Varied Microstructure. *J. Biomech. Eng.* **2002**, *124*, 214.
(38) Lungu, O. I.; Hallett, R. A.; Choi, E. J.; Aiken, M. J.; Hahn, K. M.; Kuhlman, B. Designing Photoswitchable Peptides Using the AsLOV2 Domain. *Chem. Biol.* **2012**, *19*, 507−517.
(39) Zhou, X. X.; Chung, H. K.; Lam, A. J.; Lin, M. Z. Optical control of protein activity by fluorescent protein domains. *Science (Washington, DC, U. S.)* **2012**, *338*, 810−814.
(40) Taslimi, A.; Vrana, J. D.; Chen, D.; Borinskaya, S.; Mayer, B. J.; Kennedy, M. J.; Tucker, C. L. An optimized optogenetic clustering tool for probing protein interaction and function. *Nat. Commun.* **2014**, 4925.
(41) Davidenko, N.; Schuster, C. F.; Bax, D. V.; Raynal, N.; Farndale, R. W.; Best, S. M.; Cameron, R. E. Control of crosslinking for tailoring collagen-based scaffolds stability and mechanics. *Acta Biomater.* **2015**, *25*, 131−142.
(42) Greenfield, M. A.; Hoffman, J. R.; Olvera De La Cruz, M.; Stupp, S. I. Tunable Mechanics of Peptide Nanofiber Gels. *Langmuir* **2010**, *26*, 3641−3647.

https://dx.doi.org/10.1021/acsbiomaterials.0c01488
ACS Biomater. Sci. Eng. 2021, 7, 408−414